Synthesis and Characterization of Bisthienylethene-Porphyrin Photoswitchable Copolymers

Zhaohui Huo, Vasilica-Adriana Badets, Helen Ibrahim, Michel Goldmann, Hualong Xu, Tao Yi, Corinne Boudon, Laurent Ruhlmann

Synthesis and characterization of bisthienylethene-porphyrin photoswitchable copolymers

Zhaohui Huo [a,b], Vasilica Badets [a], Helen Ibrahim [c], Michel Goldmann [c,d], Hualong Xu [e], Tao Yi [f], Corinne Boudon [a] and Laurent Ruhlmann *[a]

In memory of an extraordinary and a brilliant scientist, our friend Prof. Dr. François Diederich.

[a] Laboratoire d'Electrochimie et de Chimie Physique du Corps Solide, Institut de Chimie, UMR CNRS 7177
4 rue Blaise Pascal, CS 90032, 67081 Strasbourg
* E-mail : lruhlmann@unistra.fr
[b] Zhaohui Huo
Department of Chemistry, Guangdong University of Education
351 Xin Gang Zhong Road, 510303 Guangzhou, China
[c] Sorbonne Universités, UPMC Univ Paris 06, Institut des NanoSciences de Paris, UMR CNRS 7588,
Université Paris 6, 4 place Jussieu, boîte courrier 840, F - 75252 Paris, France
[d] Université Paris Descartes
45 rue des Saints Pères, 75006 Paris, France
[e] Department of Chemistry, Laboratory of Advanced Materials, Shanghai Key Laboratory of Molecular Catalysis and Innovative Materials and Collaborative Innovation Center of Chemistry for Energy Materials
Fudan University
220 Handan Road, 200433 Shanghai, China.
[f] Department of Chemistry and Innovation Center of Chemistry for Energy Materials
Fudan University
220 Handan Road, 200433 Shanghai, China.

Abstract: The bisthienylethene (BTE) class is one of the most intensely studied type of photochromatic dye which attract great attention from researchers seeking to exploit light responsive switches in an extensive diversity of fields. BTE is the subject of many avenues of research. We report here the synthesis of a new diarylethene-porphyrin photoswitchable copolymer via the electropolymerization of zinc octaethyl porphyrin and pyridine substituted diarylethene. The electropolymerization was monitored by electrochemical quartz crystal microbalance (EQCM). The copolymer was characterized by electrochemistry, UV-Vis spectroscopy, X-ray photoelectron spectroscopy (XPS), and atomic force microscopy (AFM). The incorporated diarylethene maintains its reversible photochromism upon the UV-Vis radiation with multiple cycles of ring-opening and closing. Attention is focused on the ways the polymer environment affects BTE photochromism.

Introduction

Diarylethenes are photochromic materials with promising potential for the development of photonic devices such as optical switches due to their reversible photocyclization reaction [1–3]. Specifically, bisthienylethene (BTE) derivatives display thermally irreversible, fast-switching, high quantum-yield and fatigue resistant photoisomerization reactions.

The photocyclization reaction are most of the times accompanied by the change of other physical-chemical properties such as refractive index, optical rotation or luminescence. Switchable supramolecular self-assemblies based on the interaction between pyridine group containing bisthienylethene unit (**BTEPy**) and carboxylic acids showed fluorescent enhancement both in solution and also in the solid state [4].

In addition, in the presence of metal ion such as Zn^{2+}, the photochromism from the open to the closed-ring form was strongly enhanced [5].

A bisthienylethene iridium (III) complex coordinating to the photochromic diarylethene derivative **BTEPy** was described. $(BTEPy)_2Ir(acac)$ showed excellent near-infrared photochromic properties such as thermal stability and fatigue resistance accompanied by efficient quenching of phosphorescence emission by the closed form of the bisthienylethene moiety [6]. Furthermore, bisthienylethene-based iridium(III) complex was used as a phosphorescence probe for monitoring living cells [7].

Porphyrins get excited at a wavelength where the open form of BTE is transparent. Moreover, the spectral overlap between the emission band of porphyrin and the closed form of BTE provides a mean to regulate the luminescence via the photoisomerization reaction [8]. The ability to control the excitation wavelengths of porphyrins and their intense luminescence far into the visible domain led to intense research of porphyrin−dithienylethene hybrids. Most of the examples cited here are based on covalent or coordinative bonds between the two molecules [9,10].

Coordination complex between Ru porphyrin and **BTEPy** was prepared showing optical switch which phosphoresces at 730 nm instead of fluorescing and consequently emits light energy far beyond the photochemically active absorption bands. The emission intensity can be modulated by photochemically switching between open and closed forms [11].

Synthesis of photochromic hybrid, where porphyrin macrocycles are attached to the ends of the bisthienylethene backbone was also described. The luminescence intensity of the porphyrin is significantly governed by the state of the bisthienylethene photoswitch. The photoisomerization reaction was carried out under illumination at 313 nm and the non-fluorescent closed form was obtained while in the open form, the porphyrins display significant fluorescence intensity at 655 nm when excited at 430 nm [8]. In bisthienylethene-bridged diporphyrins, the close attachments of the porphyrin to the bisthienylethene induced loss of its photochromic reactivity, probably through the intramolecular

energy transfer quenching. However, the appropriate selection of a spacer between the bisthienylethene and porphyrin guarantees the photochromic reactivity of the bisthienylethene moiety that can reversibly control the fluorescence of the porphyrin subunit [12].

Additionally, Moore's group prepared bisthienylethene-porphyrin–fullerene triad (BTE–porphyrin-C60) as an electron-transfer switch, which showed no significant porphyrin fluorescence in either open or closed forms [13].

These properties make from BTE a very good candidate for the development of responsive surfaces that currently receive widespread interest in applications such as microfluidic devices, sensors, organic devices and electronics [3]. The common approach to get these responsive surfaces is to incorporate a stimuli responsive unit into a polymer while keeping the functionality undisrupted.

The incorporation of BTE into polymers while keeping its thermally irreversible photochromism has been widely reported in the literature. We distinguish here the polymers obtained by the electropolymerisation of subunit of BTE backbone from polymers obtained via incorporation (e.g. in polystyrene [14] or poly(methyl methacrylate) [15]) or other chemical reactions (e.g. click chemistry [16]).

The electropolymerisation of bifunctional diarylethene substituted with methoxystyryl [17], bis-tertiophene or bis-bithiophene [18,19] and 2,5-dithienylpyrrole [20] were reported. G. Zerbi et al. synthesized a thiophene backbone photochromic polymer, whose thermal stability was surprisingly higher than that of the monomer [21].

Reaction of 2,3-bis (2,5-dimethyl-3- thienyl)-N-allyl maleimide with methyl methacrylate (MMA) gave photochromic copolymer with quite high cyclization and ring opening quantum yields, even for the copolymers in the film. The switching stability of the photochromic copolymer was observed a least during over 200 open to closed cycles [22].

Several homopolymers from 1,2-bis(3-thienyl)cyclopentene derivatives were also synthetized using ring-opening metathesis polymerization methods [23]. These homopolymers retained their photochromic properties both in solution and in the solid state. But the photochromic properties in solution diverged from those of its monomer. It is probably due to the decline in rotational freedom of the C–C bonds between the thiophene and cyclopentene rings because of the rigidity of each end of the photochromic skeleton joining the cross-linked polymer backbones. Free rotation around these bonds is indispensable to orient the orbits for the electrocyclic ring closing reaction.

In the case of the polymer based on bis-tertiophene, reversible switching of conductivity within diarylethene-based redox-active polymer films was observed [19].

Singlet oxygen generation [24], photo-patterning [25] and quenching of electron transfer from a singlet state excited porphyrin to a fullerene was also modulated by the photocyclisation reaction [26].

In this view, we present here a copolymer obtained by the electropolymerization of a porphyrin unit and BTE (Scheme 1). It is important to note that the polymer is not obtained via the direct electropolymerization of a moiety of BTE, as most of the BTE containing polymers published so far. Moreover, our material is not a simple association of one unit of porphyrin with BTE, as most of the examples cited above; it consists of a porphyrin copolymer with BTE included in the backbone and not as a pendant group.

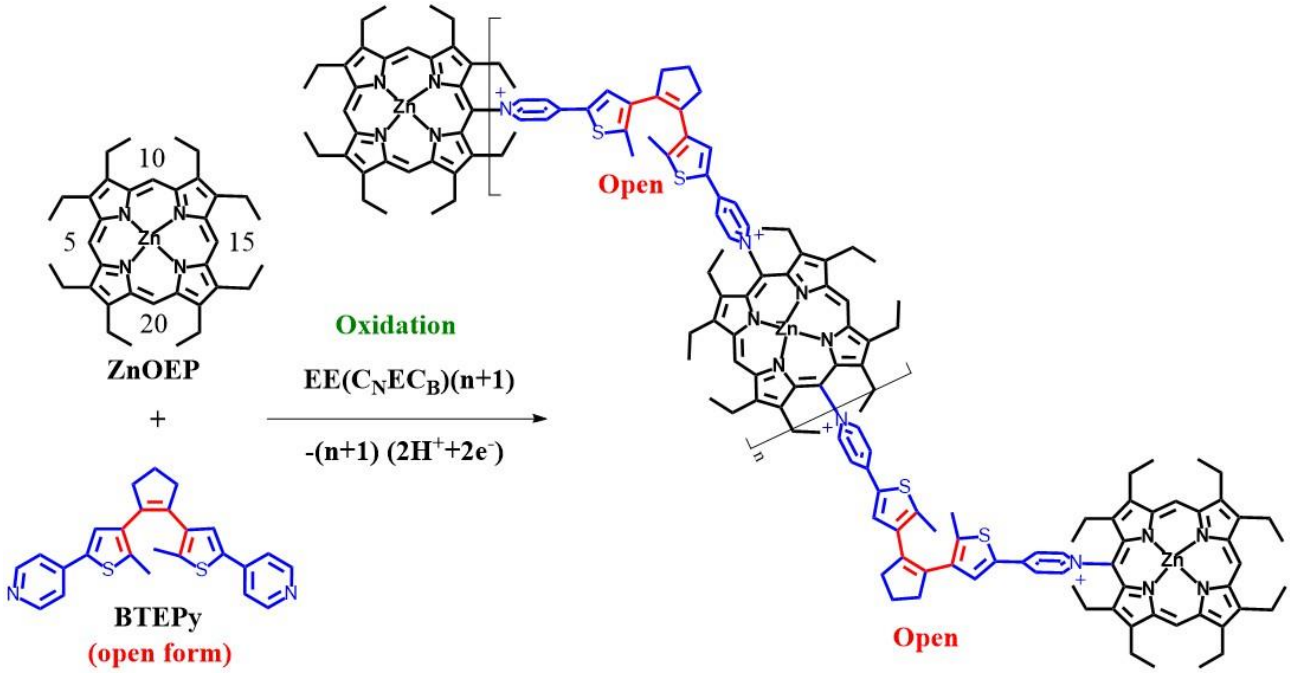

Scheme 1 General electropolymerization scheme of **ZnOEP** with **BTEPy**.

Results and Discussion

Electroynthesis of the Poly-BTEPy-ZnOEP copolymers

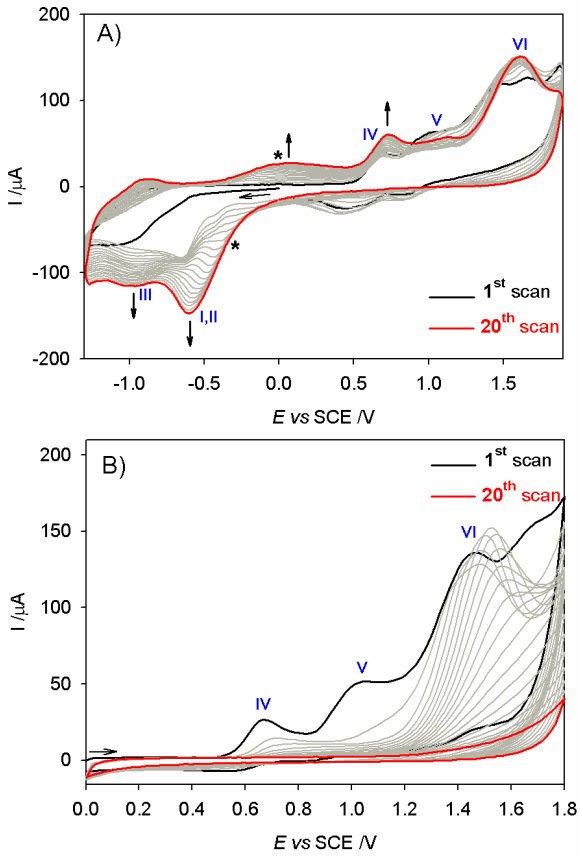

Figure 1. Cyclic voltammograms recorded A) between −1.30 V and +1.80 V vs. SCE and B) between 0.0 V and +1.80 V vs. SCE during the electropolymerization of 0.25 mmol/dm^3 **ZnOEP** with 0.25 mmol/dm^3 **BTEPy** in CH_3CN/1,2-$C_2H_4Cl_2$ (3/7) in the presence of 0.1 mol/dm^3 NBu_4PF_6. Working electrode: ITO. (←) Start of the scan. S =1 cm^2; scan rate: 0.1 V/s.

Scheme 1 presents the electropolymerization process. The principle of electropolymerization of zinc octaethyl porphyrin in the presence of pyridine containing spacers have been developed by our group and multiple examples have been published so far [27–29]. The process involves the formation of a porphyrin dication by raising the electrode potential to positive values (step V in Figure 1, above 1 V *vs.* SCE). This high electrophilic dication undergoes a nucleophilic attack from pyridine substituted compounds.

In the present work, we have tested this process using pyridine substituted diarylethene (**BTEPy**, Scheme 1). Figure 1 shows the electropolymerization process that was optimized with respect to the scan direction and lower potential limit that is either -1.3 V or 0 V *vs.* SCE. In the anodic scan, peaks corresponding to the formation of a first porphyrin radical cation (step IV into Figure 1) followed by the peak of the porphyrin dication (step V) and finally by the peak corresponding to the oxidation of isoporphyrin (step VI) are observed. In the cathodic scan down to -1.3 V (Figure 1A) peaks corresponding to the reduction of the intermediate isoporphyrin and of the pyridinium reduction (peaks *, I, II and III) are observed. The first one (peak *) could correspond to the reduction of the isoporphyrin and the three others (peaks I, II and III into Figures 1 and 3) could correspond to the reductions of the pyridinium spacers formed between each porphyrin ring and BTE. Peaks I and II are irreversible while peak III is reversible. The last wave (peak III) probably corresponds to the simultaneous reduction of the pyridinium groups substituted in 5 and 15 meso-positions of the porphyrin (bi-substitution in positions 5 and 15, i.e.

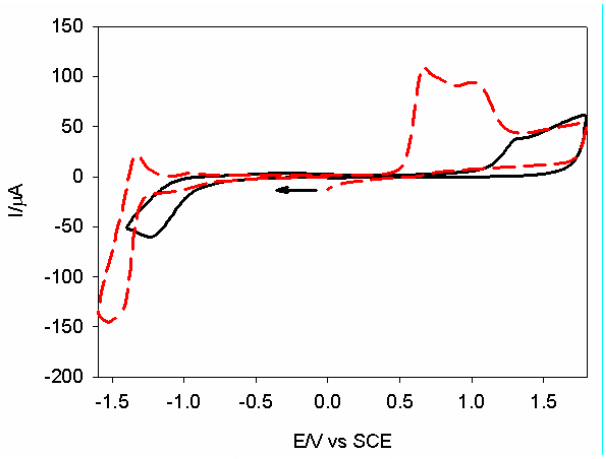

Figure 2. Cyclic voltammetry of BTEPy in the open form (black curve) and closed form (dotted red curve under illumination at λ=330 nm) in CH_3CN/1,2-$C_2H_4Cl_2$ (3/7) with 0.1 mol/dm^3 NBu_4PF_6. (←) Start of the scan. Working electrode: ITO, S =1 cm^2; scan rate: 0.1 V/s.

trans-substitutions) while the first signals (peaks I and II, observed at -0.52 V and -0.75 V *vs.* SCE) probably corresponds to the reduction of pyridinium group in 5 and 10 meso-positions (in the case of bi-substitution in positions 5 and 10, i.e. *cis*-substitutions). Indeed, in the case of *cis*-substitutions, mutual interaction between the two pyridinium substituents can be observed leading to two successive one-electron reduction steps for py$^+$-BTE-py$^+$ spacers instead of only one (two electron reduction step). Indeed, when we use ZnOEP, the four meso-positions (positions 5, 10, 15 and 20) are free, and the nucleophilic attack can occur on each of them. Thus, “zigzag” polymers can be obtained. Further details about these species can be found in our previous publications [30,31]. It is important to notice here that in Figure 1A the electropolymerization leads to an increase of the current with each scan while in Figure 1B the opposite is observed. In the second case, the obtained copolymer is less conductive but also more linear (with bi-substitution mainly in positions 5 and 15, *i.e.* trans-substitutions). For this reason, the electropolymerization between 0 and 1.8V was chosen and all the results are presented for this copolymer (further called **Poly-BTEPy-ZnOEP**).

The electrochemical behavior of **BTEPy** alone (in its open and closed form) is described in Figure 2. For the open form an irreversible oxidation and an irreversible reduction are observed at 1.47 V and -1.16 V respectively. For the closed form the electrochemical processes are shifted toward more negative potentials, rendering the oxidation of this form easier to perform. If the oxidation of **BTEPy** would be encountered during the electropolymerization, the ability to perform photoswitchable reactions might be altered. For this reason, the open form was selected for performing the electropolymerization.

Cyclic voltammetric investigations of the films

Figure 3 shows the electrochemical behavior of the final copolymer **Poly-BTEPy-ZnOEP** and Table 1 contains a summary of peak position for all the species present in the copolymer or as standalone species.

Table 1. Electrochemical data for **ZnOEP**, **BTEPy** and **Poly-BTEPy-ZnOEP.**

Compounds	Ring oxidation		Reduction of py^+	Ring reduction
ZnOEP [a]	1.08 (130)	0.71 (128)		-1.66
BTEPy [b]	1.47			-1.16
Poly-BTEPy-ZnOEP [c]			-0.11* (190), -0.52 (irr (peak I)), -0.75 (irr (peak II)), -0.85 (peak III) (92)	

Peak *: reduction of the isoporphyrin intermediate.

[a] Potentials in V *vs.* SCE were obtained from cyclic voltammetry in 1,2-$C_2H_4Cl_2$ with 0.1 mol/dm^3 NBu_4PF_6. Scan rate = 100 mV s^{-1}. Working electrode: ITO, S=1 cm^2.

[b] Open form of **BTEPy**. Potentials in V *vs.* SCE were obtained from cyclic voltammetry measured in the dark in CH_3CN with 0.1 mol/dm^3 NBu_4PF_6. Scan rate = 100 mV s^{-1}. Working electrode: ITO, S=1 cm^2.

[c] Potentials in V *vs.* SCE were obtained from cyclic voltammetry in CH_3CN/1,2-$C_2H_4Cl_2$ (3/7) with 0.1 mol/dm^3 NBu_4PF_6. Scan rate = 100 mV s^{-1}. Working electrode: ITO, S=1 cm^2. The given half-wave potentials are equal to $E_{1/2} = (E_{pa} + E_{pc})/2$. Under bracket: $\triangle E_p = |E_{pa}-E_{pc}|$.

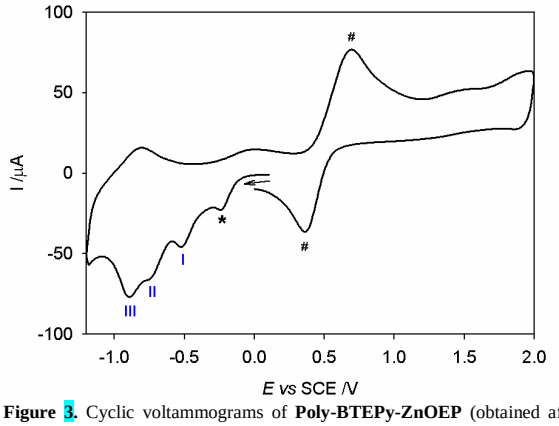

Figure 3. Cyclic voltammograms of **Poly-BTEPy-ZnOEP** (obtained after 50 scans, between 0.00 V and +1.80 V) in CH_3CN/1,2-$C_2H_4Cl_2$ (3/7) with 0.1 mol/dm^3 NBu_4PF_6. (←) Start of the scan. S =1 cm^2; scan rate: 0.1 V/s. Peak #: Fc/Fc^+ internal reference. Peak *: reduction of the isoporphyrin.

Inside the copolymer, specific peaks of pyridinium (py^+) reduction are observed. No signals of the **BTEPy** (included in the copolymer) are observed because the oxidation and reduction process are largely diminished once the species is entrapped in the polymer.

The electropolymerization process was followed also via an electrochemical quartz crystal microbalance in order to measure the deposited amount. Figure 4 shows the increasing deposited mass with each scanning cycle. A total value of 3.2 µg.cm^{-2} was deposited after 50 scanning cycles.

Film morphology (atomic force microscopy)

The deposited film was also studied by scanning atomic force microscopy (AFM) (Figure 5). From Figure 5, it can be seen that

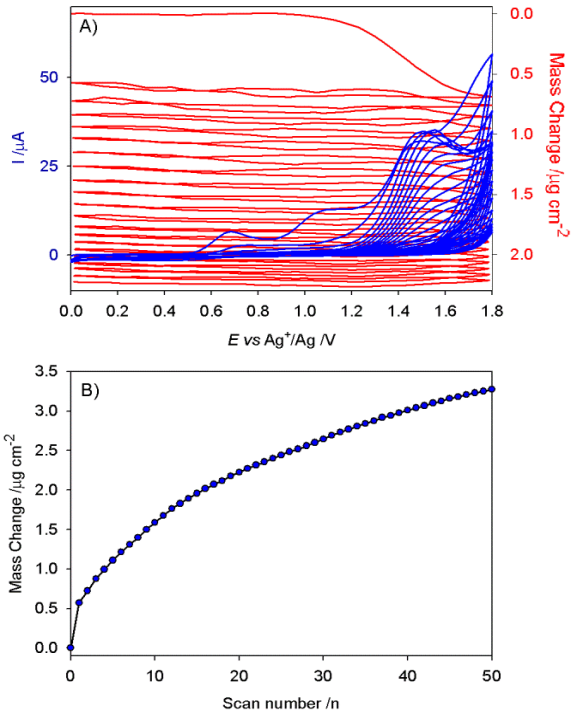

Figure 4. A) Consecutive cyclic voltammograms and electrochemical quartz crystal microbalance measurements for the first 20 scans during the electropolymerization of 0.25 mmol/dm^3 **BTEPy** with 0.25 mmol/dm^3 **ZnOEP** in CH_3CN/1,2-$C_2H_4Cl_2$ (3/7) in the presence of 0.1 mol/dm^3 NBu_4PF_6. Working electrode: ITO (A = 0.2 cm^2) deposited on a 9.08 MHz AT-cut quartz crystal. v = 100 mV s^{-1}. B) Mass change (Δm) calculated from Sauerbrey's equation *versus* the number of scan n.

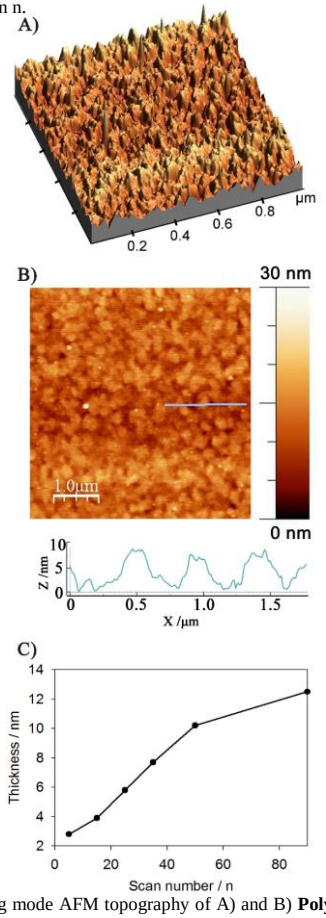

Figure 5. Tapping mode AFM topography of A) and B) **Poly-BTEPy-ZnOEP** films (obtained after 50 scans, between 0.00 V and +1.80 V) and section analysis of the aggregate marked by a cyan line for B). C) Thickness measured by AFM versus different numbers of iterative scans.

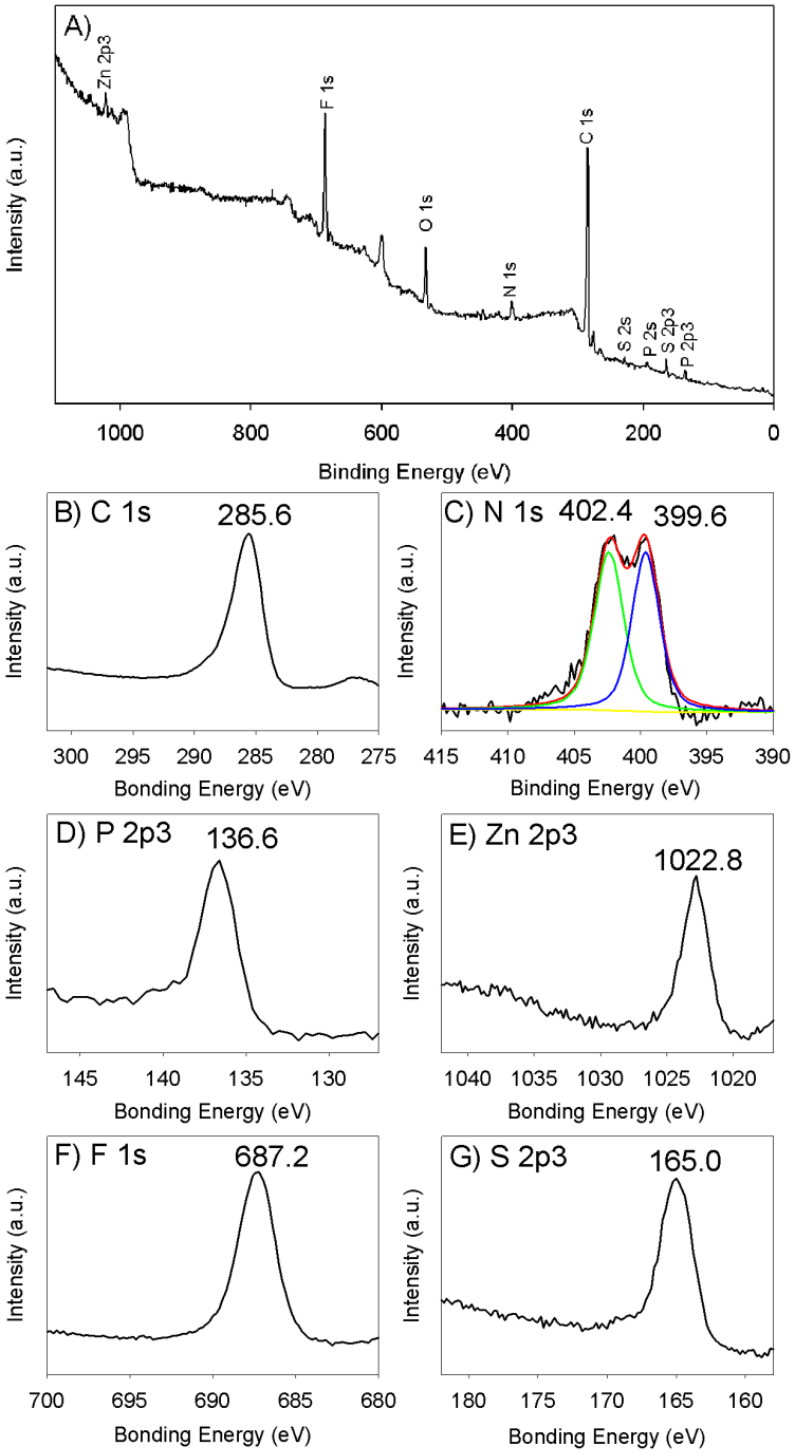

Figure 6. XPS spectra of the modified ITO electrodes with Poly-BTEPy-ZnOEP obtained after 25 iterative scans between 0.00 and +1.80 V vs. SCE. (A) Global XPS spectra, (B) C 1s, (C) N 1s, (D) P 2p3, (E) Zn 2p3, (F) F1s, (G) S 2p3.

the deposit shows packed aggregates. Tightly packed aggregated coils of the copolymer appear on the surface with an average diameter of ca. 200-300 nm. The deposited thickness varies with the number of scans, reaching 10 nm after 50 scanning cycle.

The rms surface roughness of the **Poly-BTEPy-ZnOEP** film has been estimated at 3.3 nm (calculated from an area of 1 μm^2).

The presence of tightly packed aggregated may be due to π-π interactions, in particular between porphyrin macrocycles.

X-ray photoelectron spectroscopy (XPS)

The copolymer films were also investigated by X-Ray photoelectron spectroscopy (Figure 6).

XPS data revealed the presence of **BTEPy** in the final copolymer due to signal of sulfur S 2p3 at 165.0 eV, along with signals characteristic to the **ZnOEP** based copolymer described elsewhere [30-31].

The analysis of the survey spectra of **Poly-BTEPy-ZnOEP** confirms the presence of the porphyrin subunits (Zn 2p3 at 1022.8 eV, C 1s, 285.6 eV and N 1s peaks). The N1s peaks reveal the

presence of two chemically different nitrogen atoms. The contributions at 402.4 eV and 399.6 eV are attributed to the iminic nitrogen and to the reduced pyridinium respectively.
Furthermore, the signals of phosphorus 2p3 (136.6 eV) as well as fluorine 1s (687.2 eV) correspond to the PF_6^- counter-anion also present in the copolymer.

UV-visible spectroscopy and photoisomerization reaction

Table 2. UV–visible spectral data for **ZnOEP** and **BTEPy** in DMF, **Poly-BTEPy-ZnOEP** on ITO and in DMF. In brackets: molar extinction coefficient (ε /10^3 $dm^3 \cdot mol^{-1} \cdot cm^{-1}$).

Compound	Soret band/nm	Q bands/nm	π-π* Band/nm
ZnOEP	408 (672.3)	538 (34.3) 674 (37.7)	
BTEPy			283 (21.3), 320 (14.4)
Poly-BTEPy-ZnOEP (ITO)	425	554, 588	
Poly-BTEPy-ZnOEP (DMF)	421	547, 586	269

The optical properties of **Poly-BTEPy-ZnOEP** were recorded during UV-Vis experiments. Figure 7A presents the UV-Vis spectra as a function of the number of scanning cycles while Figure 7B shows a comparison between the UV-Vis spectra of **ZnOEP** alone, **BTEPy** alone as well as the polymer as obtained on ITO electrodes and the polymer dissolved in dimelthylformamide. Table 2 contains a summary of the absorption bands. It is important to notice that the **Poly-BTEPy-ZnOEP** displays mainly the specific band of the porphyrin when immobilized on ITO and it displays also the specific band of **BTEPy** while dissolved in DMF.

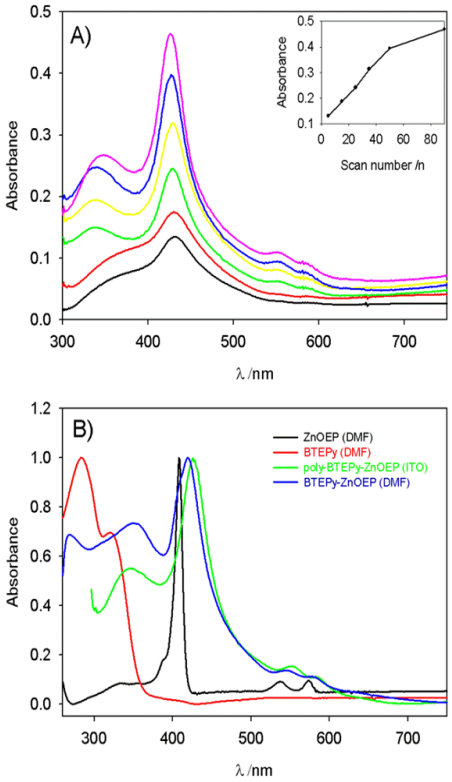

Figure 7. A) UV–vis absorption spectra of **Poly-BTEPy-ZnOEP** (obtained after n iterative scans, between 0.00 V and +1.80 V) on ITO. B) UV–vis normalized absorption spectrum of **Poly-BTEPy-ZnOEP** (obtained after 25 iterative scans) onto ITO electrode (green line) or in DMF solution (blue line) compared to **ZnOEP** (black line) and **BTEPy** (red line) in DMF.

Please note that a quantitative quenching of the emission of the porphyrin for **Poly-BTEPy-ZnOEP** has been measured.
The most important information of this paper is the ability of **BTEPy** to undergo its specific photoisomerization reactions inside

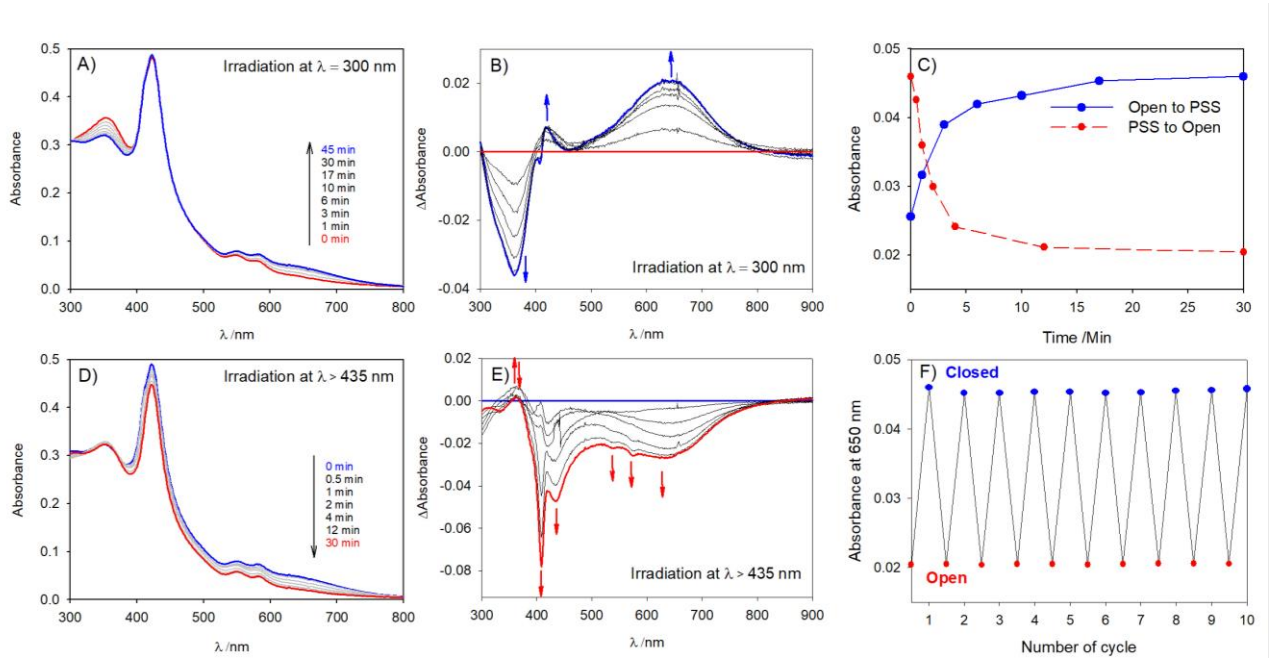

Figure 8. A) UV-vis absorption spectral changes of **Poly-BTEPy-ZnOEP** (open-ring form to PSS) in DMF under different irradiation time by light at λ = 300nm and B) the corresponding differential spectra. C) Absorbance evolution at λ = 650 nm during the process A) and D). D) UV-vis absorption spectral changes of **Poly-BTEPy-ZnOEP** (PSS to open-ring form) in DMF under different irradiation time by light λ > 435 nm and E) the corresponding differential spectra. F) Absorbance evolution at λ = 650 nm during repetitive cycles to convert **Poly-BTEPy-ZnOEP** from open to closed form.

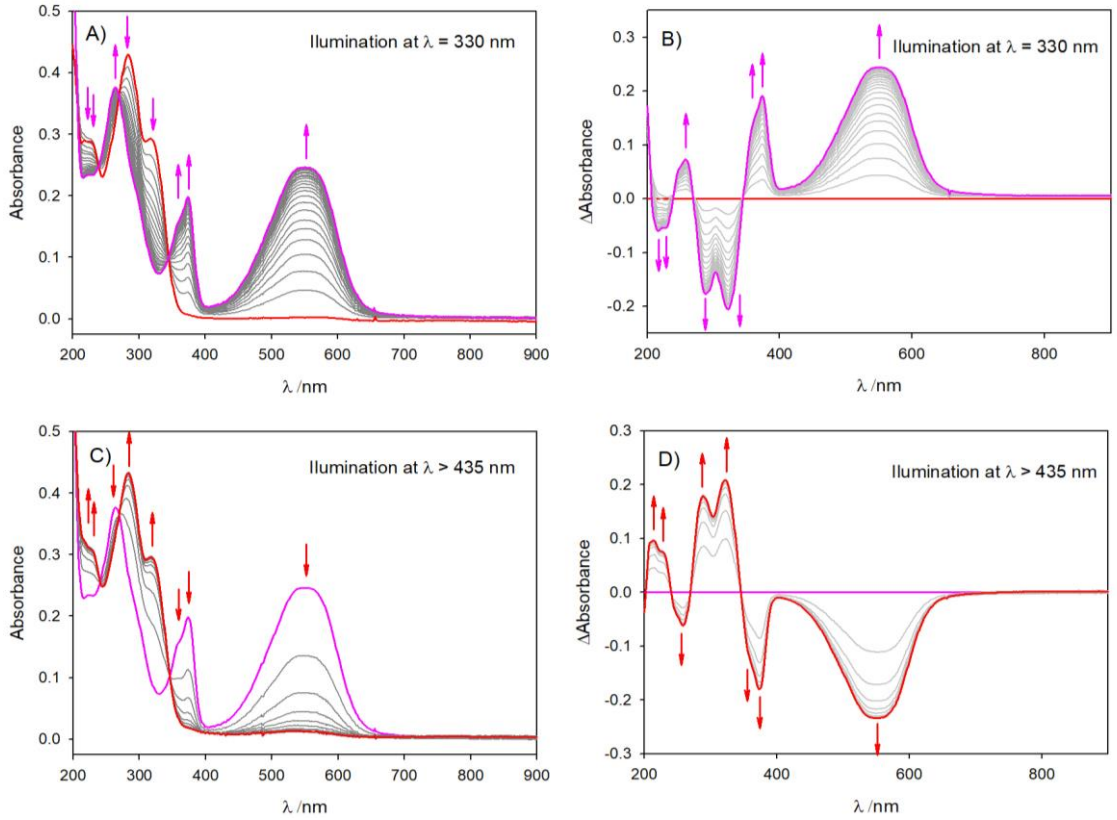

Figure 9. UV-vis absorption spectral changes of **BTEPy** (open-ring form to PSS) in CH_3CN under different irradiation time by light λ = 330 nm and B) the corresponding differential spectra. C) UV-vis absorption spectral changes of **BTEPy** (PSS to open-ring form) in DMF under different irradiation time by light λ > 435 nm and D) the corresponding differential spectra. C = $1.5.10^{-5}$ mol/dm^3.

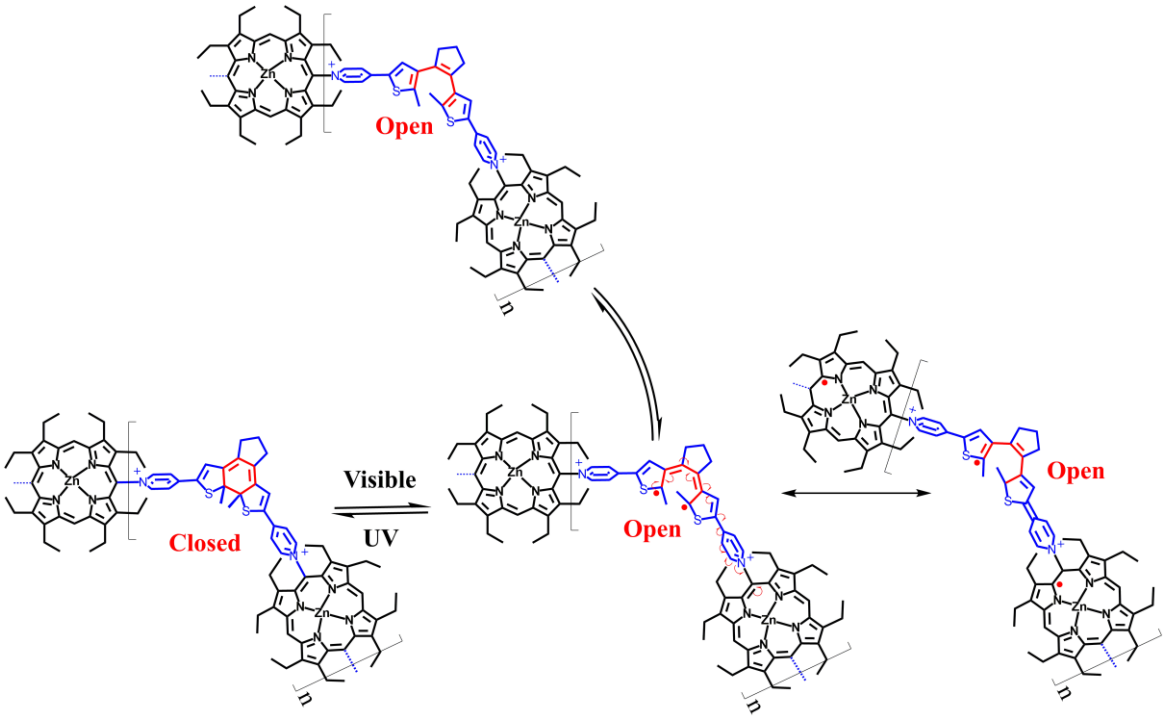

Scheme 2. Open to closed interconversion of **Poly-BTEPy-ZnOEP**.

the copolymer backbone (Scheme 2). Figure 8 shows the changes of UV-Vis spectra under the illumination at a wavelength of 300 nm followed by an illumination at a wavelength higher than 435 nm for **Poly-BTEPy-ZnOEP** dissolved in DMF. The changes of the UV-Vis spectra are specific to the switch from the open form to the photostationary stare (PSS) and vice-versa. The differential spectra (subtraction of the initial spectrum from the spectrum at t) confirms the photoconversion from the open to closed form with

the appearance of bands around 640 nm and 410 nm and the decrease in the initial band around 360 nm (Figure 8B).
Compound closed-**Poly-BTEPy-ZnOEP** is stable at room temperature, but can be reverted back to open-**Poly-BTEPy-ZnOEP** by visible irradiation (Figures 8DE). The differential spectra show the disappearance of bands around 640 nm and 410 nm. It confirms the photoisomerization from the closed to the open form.
However, the recovering in the initial band around 360 nm is partial. It must be also noticed that a slight decrease of the bands associated to the **ZnOEP** porphyrin (Soret and Q bands) are observed during illumination (Figure 8E) which may indicate the formation of the radical **ZnOEP•** porphyrin which breaks the aromaticity of the macrocycle inducing the decrease of the intensity of the bands associated to the porphyrin
These results suggest that during the photoisomerization reaction from the closed to the open form, the radicals formed can be at least partially delocalized to the porphyrin macrocycle (Scheme 2).

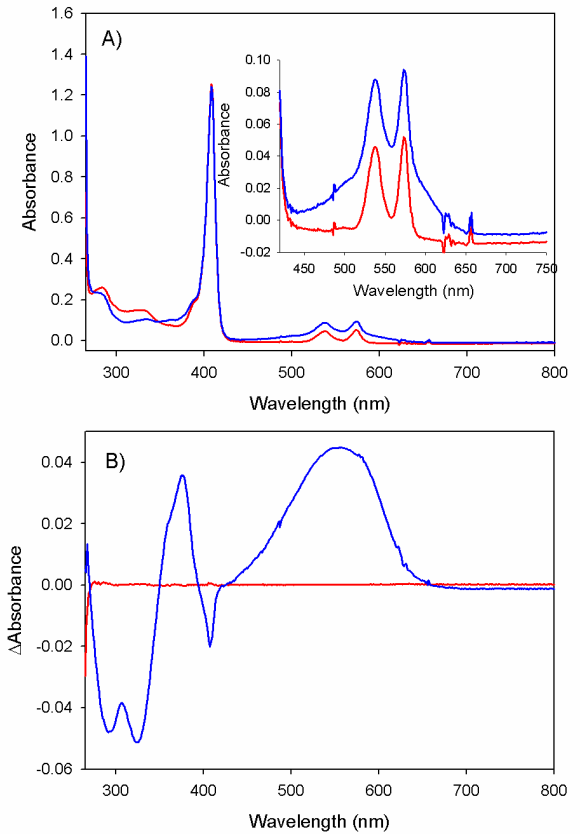

Figure 10. UV-vis absorption spectral changes of the mixture **ZnOEP** + **BTEPy** (open-ring form to PSS) in DMF under illumination at λ = 330 nm during 10 minutes and B) the corresponding differential spectrum. C = 0.375.10^{-5} mol/dm^3.

The ability of **BTEPy** alone to perform the photoisomerization reactions was also measured during the UV-Vis experiments performed in the same condition (Figure 9), proving that BTE behavior is not altered by attached pyridine. A model mixture ZnOEP/BTEPy (1/1) for a solution comparison has been also studied in DMF showing similar behavior than for **BTEPy** alone in solution has been observed as expected (Figure 10).
Nevertheless, it is worthwhile to mention here that the copolymer **Poly-BTEPy-ZnOEP** cannot perform the photoisomerization reactions while immobilized onto ITO electrode. This result diverges with homopolymers obtained from 1,2-bis(3-thienyl)cyclopentene [23] which retain their photochromic properties both in solution and in the solid state. It can be explained by the presence of π-π interactions as well as electrostatic interactions between the pyridinium and the PF_6^- counteranions in the copolymer (aggregated coils observed by AFM, Figure 5).
Note that it takes about 30 minutes to perform the photoisomerization reactions from the open to closed form and reach the plateau in the case of **Poly-BTEPy-ZnOEP** polymer. In the case of **BTEPy**, the time required for the photocyclisation under the same experimental conditions was 5 minutes. This result can easily be explained for the polymer by the decrease in rotational freedom around the C–C bonds between the thiophene and cyclopentene rings because of the rigidity of each end of the photochromic skeleton joining the cross-linked polymer backbones, namely the porphyrins and the pyridinium.
High reversibility of the interconversion open – closed form has been observed during repetitive switching cycles consisting of alternating UV-visible and visible irradiation (Figure 8F) and no spontaneous cycloreversion can be observed at room temperature.

Conclusion

In conclusion, we have demonstrated here the possibility to obtain a porphyrin based copolymer including bisthienylethene units. The copolymer is able to perform photoswitchable isomerization reactions, proving that the incorporation of **BTEPy** was successful. This is a proof of concept and further associations of porphyrin and **BTEPy** are currently under development in our group.

Experimental Section

Most common laboratory chemicals were reagent grade, purchased from commercial sources and used without further purification. The zinc-*β*-octaethylporphyrin (**ZnOEP**) was purchased from Sigma-Aldrich. The pyridine substituted diarylethene, (1,2-Bis[2-methyl-5-(4-pyridyl)-3-thienyl]cyclo-pentene, abbreviated **BTEPy**) was synthesized according to the litterature [4]. ^{1}H NMR (400 MHz, $CDCl_3$) δ (ppm) 8.51 (d, 6 Hz, 4H, pyridyl *α*-H), 7.33 (d, J=6.4 Hz, 4H, pyridyl *β*-H), 7.21 (s, 2H, thienyl C–H), 2.84 (t, 4H, $–CH_2–$), 2.10 (m, 2H, $–CH_2–$), 2.01 (s, 6H, $–CH_3$).
Voltammetric data have been recorded with a standard three-electrode system using a PARSTAT 2273 potentiostat.
Electropolymerizations have been carried out under an argon atmosphere using a 0.1 mol/dm^3 solution of 0.1 mol/dm^3 $TBAPF_6$ in 1,2-$C_2H_4Cl_2$/CH_3CN (7/3) containing 0.25 mmol/dm^3 of **ZnOEP** and 0.25 mmol/dm^3 of **BTEPy** (Scheme 1) between 0 or -1.3 and 1.8 V *vs.* SCE. Single-side coated indium-tin-oxide (ITO, SOLEMS, 25–35 Ω/cm^2) electrodes with a surface area of 1 cm^2 were used as working electrode, and a platinum wire as auxiliary electrode. The reference electrode was the saturated calomel electrode which was electrically connected to the solution by a junction bridge filled with electrolyte. For each copolymer, the number of iterative scans (n) was 20. After electropolymerization,

the modified working electrodes were washed with CH_3CN and then with CH_2Cl_2 in order to remove the monomers and the conducting salt present on the deposited films.
The electrochemically deposited films were dissolved and removed from ITO electrode with DMF. The operation is repeated 6 times.
UV–vis absorption spectra were recorded with a single beam Hewlett-Packard HP 8453 diode array spectrophotometer operated at a resolution of 2 nm.
A QCA-922 (SEIKO EG&G instrument) system combined with Versa STAT 3 was used for simultaneous electrochemical quartz crystal measurement (EQCM) and cyclic voltammetric measurements. The electrochemical cell was assembled in a glove box using an ITO AT-cut quartz crystal resonator (mirror finished, resonant frequency: 9.08 MHz ± 50 kHz, A = 0.2 cm2, SEIKO EG&G., LTD) as working electrode, a platinum wire as counter electrode, and a Ag/AgCl wire as a quasi-reference electrode. The solution used for the electropolymerization here is the same as the one used for electropolymerization of the copolymers with the larger ITO electrode. Iterative scans were conducted at a scan rate of 100 $mV \cdot s^{-1}$ at room temperature with simultaneous recording of the quartz resonance frequency. The change of the quartz resonance frequency (Δf) was converted into the mass change (Δm) by applying Sauerbrey's equation (eq 1):

$$\Delta f = -2f_0^2 \Delta m / A(\mu.\rho)^{1/2} \quad (1)$$

where f_0 is the resonant frequency of the fundamental mode, ρ is density of the crystal (2.684 g/cm3), A is working area (0.2 cm2) of the ITO quartz crystal resonator, μ is shear modulus of quartz ($2.947 \times 1011\ g \cdot cm^{-1} \cdot s^{-2}$).
XPS experiments were carried out on a RBD upgraded PHI-5000C ESCA system (Perkin-Elmer) with MgKR radiation (h=1253.6 eV) or Al KR radiation (h= 1486.6 eV). In general, the X-ray anode was run at 250W and the high voltage was kept at 14.0 kV with a detection angle at 54°. The pass energy was fixed at 23.5, 46.95, or 93.90 eV to ensure sufficient resolution and sensitivity. The base pressure of the analyzer chamber was about 5×10-8 Pa. The sample was directly pressed to a self-supported disk (10 x 10 mm) and mounted on a sample holder then transferred into the analyzer chamber. The whole spectra (0-1100 eV) and the narrow spectra of all the elements with higher resolution were both recorded by using RBD 147 interface (RBD Enterprises, U.S.A.) through the Auger Scan 3.21 software. Binding energies were calibrated by using the containment carbon (C1s = 284.6 eV). The data analysis was carried out by using the RBD Auger Scan 3.21 software provided by RBD Enterprises or XPS Peak 4.1 provided by Raymund W.M. Kwok (The Chinese University of Hongkong, China).
Atomic force micrographs (AFM) measurements have been conducted directly on the ITO surfaces using a Dimension 3100 (Veeco) in the tapping mode under ambient conditions. Silicon cantilevers (Veeco probes) with a spring constant of 300 N/m and a resonance frequency in the range of 120–139 kHz have been used. The scanning rate was 1.0 Hz.
Irradiation was performed using a 300 W Xe arc lamp (Lot, Quantum design) with intense focused output beams (50 mm beam diameter) equipped with a water cell filter to absorb the IR radiation. A spherical reflector collects the output from the rear of the lamp and focuses it on or near the arc for collection by the condenser. One condenser is positioned for compensating focal length change due to dispersion and to produce a beam converging to the photochemical cell. Filter at 300 nm and long pass filter at λ > 435 nm have been used. According to the supplier, the irradiance of the lamp from 435 nm to 800 nm was around 50 $mW.m^{-2}.nm^{-1}$.

Acknowledgements

We thank CNRS, the Université de Strasbourg (France), Université Paris-Descartes (Paris, France), Sorbonne Université (Paris, France), and Fudan University (Shanghai, China) for funding of this work. The authors are grateful to the CNRS for constant financial support. We also thank the Oversea Study Program of Guangzhou Elite Project (GEP) for the Ph.D. grant of Zhaohui Huo. This work was also supported by Fund of senior visiting professor of Fudan University.

Conflict of Interest

The authors declare no conflict of interest

Keywords: Electropolymerization • Porphyrin • Bisthienylethene • Polymer • Photocyclisation

[1] M. Irie, *Chem. Rev.* **2000**, *100*, 1685–1716.
[2] H. Tian, S. Yang, *Chem. Soc. Rev.* **2004**, *33*, 85–97.
[3] M. Irie, T. Fukaminato, K. Matsuda, S. Kobatake, *Chem. Rev.* **2014**, *114*, 12174–12277.
[4] S. Xiao, Y. Zou, J. Wu, Y. Zhou, T. Yi, F. Li, C. Huang, *J. Mater. Chem.* **2007**, *17*, 2483–2489.
[5] B. Qin, R. Yao, X. Zhao, H. Tian, *Org. Biomol. Chem.* **2003**, *1*, 2187–2191.
[6] W. Tan, Q. Zhang, J. Zhang, H. Tian, *Org. Lett.* **2009**, *11*, 161–164.
[7] W. Tan, J. Zhou, F. Li, T. Yi, H. Tian, *Chem. Asian J.* **2011**, *6*, 1263-1268.
[8] T. B. Norsten, N. R. Branda, *J. Am. Chem. Soc.* **2001**, *123*, 1784–1785.
[9] H. Tian, B. Chen, H.-Y. Tu, K. Müllen, *Adv. Mater.* **2002**, *14*, 918–923.
[10] J. K. Hee, H. J. Joon, H. Choi, T. Lee, J. Ko, M. Yoon, H. J. Kim, *Inorg. Chem.* **2008**, *47*, 2411–2415.
[11] T. B. Norsten, N. R. Branda, *Adv. Mater.* **2001**, *13*, 347–349.
[12] A. Osuka, D. Fujikane, H. Shinmori, S. Kobatake, M. Irie, *J. Org. Chem.* **2001**, *66*, 3913–3923.
[13] P. A. Liddell, G. Kodis, A. L. Moore, T. A. Moore, D. Gust, *J. Am. Chem. Soc.* **2002**, *124*, 7668–7669.
[14] J. Thurn, J. Maier, M. Pärs, K. Gräf, M. Thelakkat, J. Köhler, *Phys. Chem. Chem. Phys.* **2017**, *19*, 26065–26071.
[15] S. Murase, M. Teramoto, H. Furukawa, Y. Miyashita, K. Horie, *Macromolecules* **2003**, *36*, 964–966.
[16] R. Singh, H.-Y. Wu, A. K. Dwivedi, A. Singh, C.-M. Lin, P. Raghunath, M.-C. Lin, T.-K. Wu, K.-H. Wei, H.-C. Lin, *J. Mater. Chem. C* **2017**, *5*, 9952–9962.
[17] P. Wesenhagen, J. Areephong, T. Fernandez Landaluce, N. Heureux, N. Katsonis, J. Hjelm, P. Rudolf, W. R. Browne, B. L. Feringa, *Langmuir* **2008**, *24*, 6334–6342.
[18] L. Kortekaas, W. R. Browne, *Adv. Opt. Mater.* **2016**, *4*, 1378–1384.
[19] H. Logtenberg, J. H. M. van der Velde, P. de Mendoza, J. Areephong, J. Hjelm, B. L. Feringa, W. R. Browne, *J. Phys. Chem. C* **2012**, *116*, 24136–24142.
[20] M. P. Algi, A. Cihaner, F. Algi, *Tetrahedron* **2014**, *70*, 5064–5072.
[21] C. Bertarelli, M. C. Gallazzi, F. Stellacci, G. Zerbi, S. Stagira, M. Nisoli, S. De Silvestri, *Chem. Phys. Lett.* **2002**, *359*, 278–282.
[22] H. Tian, H.-Y. Tu, *Adv. Mater.* **2000**, *12*, 1597–1600.
[23] A. J. Myles, N. R. Branda, *Macromolecules* **2003**, *36*, 298–303.
[24] L. Hou, X. Zhang, T. C. Pijper, W. R. Browne, B. L. Feringa, *J. Am. Chem. Soc.* **2014**, *136*, 910–913.
[25] T. Biellmann, A. Galanti, J. Boixel, J. A. Wytko, V. Guerchais, P. Samorì, J. Weiss, *Chem. – Eur. J.* **2018**, *24*, 1631–1639.
[26] J. Frey, G. Kodis, S. D. Straight, T. A. Moore, A. L. Moore, D. Gust, *J. Phys. Chem. A* **2013**, *117*, 607–615.
[27] I. Azcarate, I. Ahmed, R. Farha, M. Goldmann, X. Wang, H. Xu, B. Hasenknopf, E. Lacôte, L. Ruhlmann, *Dalton Trans.* **2013**, *42*, 12688–12698.

[28] Z. Huo, D. Zang, S. Yang, R. Farha, M. Goldmann, B. Hasenknopf, H. Xu, L. Ruhlmann, *Electrochimica Acta* **2015**, *179*, 326–335.
[29] Z. Huo, A. Bonnefont, Y. Liang, R. Farha, M. Goldmann, E. Saint-Aman, H. Xu, C. Bucher, L. Ruhlmann, *Electrochimica Acta* **2018**, *274*, 177–191.
[30] D. Schaming, I. Ahmed, J. Hao, V. Alain-Rizzo, R. Farha, M. Goldmann, H. Xu, A. Giraudeau, P. Audebert, L. Ruhlmann, *Electrochimica Acta* **2011**, *56*, 10454–10463.
[31] M. Boudiaf, Y. Liang, R. Lamare, J. Weiss, H. Ibrahim, M. Goldmann, E. Bentouhami, V. Badets, S. Choua, N. Le Breton, A. Bonnefont, L. Ruhlmann, *Electrochimica Acta* **2019**, *309*, 432–449.

Entry for the Table of Contents

Insert graphic for Table of Contents here. ((Please ensure your graphic is in **one** of following formats))

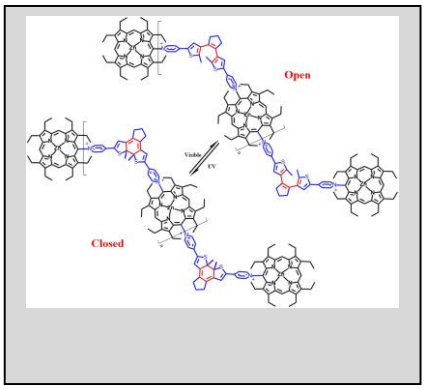

Insert text for Table of Contents here.

The synthesis of a new diarylethene-porphyrin photoswitchable copolymer via the electropolymerization of zinc octaethyl porphyrin and pyridine substituted diarylethene is reported. The incorporated diarylethene maintains its reversible photochromism upon the UV-Vis radiation with multiple cycles of ring-opening and closing.